Supporting Information cover sheet

Cost-efficiency trade off and the design of thermoelectric power generators

Kazuaki Yazawa and Ali Shakouri

University of California Santa Cruz, Santa Cruz, California, 95064 USA

Summary of the information
Number of pages: 11
Number of figures: 6
Number of tables: 0

NOMENCLATURE

A: Area [m^2]

a: Effective width of TE leg [m^2]

C_p: Specific heat [W/mK]

D: Width of heat sink or channel [m]

d: Leg length [m]

F: Fill factor (fractional area coverage of TE element)

I: Current [A]

L: Length of fluid passage in heat sink or channel [m]

m: Resistance ratio [ohm/ohm]

q: Heat flow [W/m^2]

R: Electrical resistance [ohm]

S: Seebeck coefficient [V/K]

T: Temperature [K]

U: Heat transfer coefficient [W/m2K]

u: Fluid flow speed [m/s]

w: Power per unit area [W/m^2]

Z: Figure of merit [1/K]

GREEK SYMBOLS

β: Thermal conductivity [W/mK]

κ: Thermal resistance ratio [(K/W)/(K/W)]

ϕ: Spreading angle [deg]

η: Efficiency

λ: Normalized thickness of substrate ($=d_s/a$)

ρ: Density [kg/m^3]

σ: Electrical conductivity [S]

ψ: Thermal resistance [K/W]

SUBSCRIPTS

a: ambient

b: substrate

BASE: heat sink footprint

c: cold side

fin: fins or channel walls

f: fluid

h: hot side

HS: heat sink

pp: pumping power for fluid

s: source

sh; substrate hot side

sc: substrate cold side

FULL OPTIMIZATTION OF ELECTRO THERMAL SYSTEM

We have developed a generic model for a thermoelectric module taking into account external finite thermal resistances with hot and cold reservoirs. The system is defined as a thermal network shown in Fig. 1, which represents the unit configuration with a single thermoelement with substrates on both sides and external thermal resistances with the reservoirs. The resistances in the figure, in analogy with electric circuit, represent the thermal resistances, the current represents the heat flow, and the electric potential is equivalent to the temperature. Geometry of the thermoelement is optimized considering spreading or constriction thermal resistances on both hot and cold sides. A fractional area coverage $\boldsymbol{F}$ (fill factor) defines the ratio of the thermoelement cross sectional area to the substrate area. If the fill factor is equal to 1, thermal resistances $\boldsymbol{\psi_{sh}}$ and $\boldsymbol{\psi_{sc}}$ are equal to the inverse of the substrate thermal conductance. Electric potential generated by the thermoelement induces electric current flow when an external load is connected to the electrodes. In the thermal network, generated electrical current creates additional heat transport known as Peltier effect and produces Joule heat in the element. Both are described as current (heat) sources at the terminals while the element is considered as a thermal resistor.

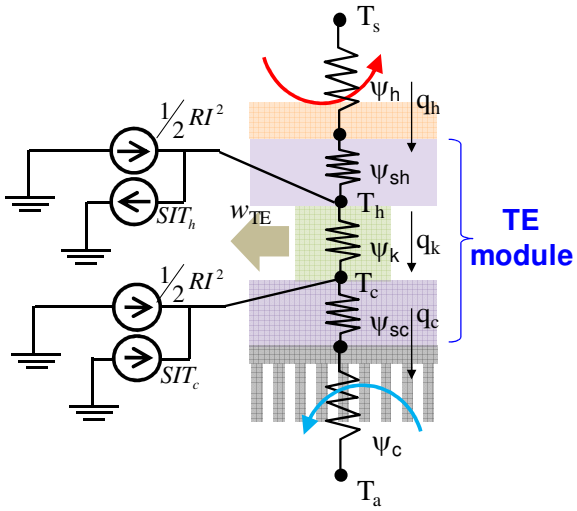

Fig. S1. Thermal network model

Thermal or electrical current distribution inside the element is not considered in this model. Heat flow balance at the two nodes $\boldsymbol{T_h}$ and $\boldsymbol{T_a}$ can be expressed as the following:

$$\frac{1}{\psi_k}(T_h - T_c) = \frac{1}{\psi_h + \psi_{sh}}(T_s - T_h) - SIT_h + \frac{I^2 R}{2} \tag{S1}$$

$$\frac{1}{\psi_c + \psi_{sc}}(T_c - T_a) = \frac{1}{\psi_k}(T_h - T_c) + SIT_c + \frac{I^2 R}{2} \tag{S2}$$

where $\boldsymbol{T_h}$ is the hot side thermoelement temperature, $\boldsymbol{T_c}$ is the cold side thermoelement temperature. $\boldsymbol{T_s}$ is the heat source temperature, and $\boldsymbol{T_a}$ is the ambient temperature. The internal thermal resistance $\boldsymbol{\psi_k}$ and the internal electrical resistance $\boldsymbol{R}$ of thermoelement (leg) are given by

$$\psi_k = \frac{d}{\beta FA},\ R = \frac{d}{\sigma FA}. \tag{S3}$$

where $\boldsymbol{A}$ is area of the substrate, $\boldsymbol{d}$ is leg length, $\boldsymbol{\beta}$ is thermal conductivity of the thermoelement and $\boldsymbol{\sigma}$ its electrical conductivity.

The material figure-of-merit ($\boldsymbol{Z}$ factor [1/K]) of TE is commonly described as,

$$Z = \frac{\sigma S^2}{\beta} \tag{S4}$$

By introducing $\boldsymbol{m}$: ratio of the external load resistance to the internal (leg) resistance, electrical current throughout the circuit $\boldsymbol{I}$ is found as,

$$I = \frac{S(T_h - T_c)}{(1+m)R} = \frac{\sigma SFA}{(1+m)d}(T_h - T_c) \tag{S5}$$

Substituting Eq. (S5) for $\boldsymbol{I}$ in the Eq. (S1) and Eq. (S2) with defining $\Psi_h = \psi_h + \psi_{sh}$ and $\Psi_c = \psi_c + \psi_{sh}$,

$$\frac{1}{\psi_k}(T_h - T_c) = \frac{1}{\Psi_h}(T_s - T_h) - \frac{\sigma S^2 FA}{(1+m)d}T_h(T_h - T_c) + \frac{\sigma S^2 FA}{(1+m)^2 d}\frac{(T_h - T_c)^2}{2} \tag{S6}$$

$$\frac{1}{\Psi_c}(T_c - T_a) = \frac{1}{\psi_k}(T_h - T_c) + \frac{\sigma S^2 FA}{(1+m)d}T_c(T_h - T_c) + \frac{\sigma S^2 FA}{(1+m)^2 d}\frac{(T_h - T_c)^2}{2} \tag{S7}$$

Thus, transforming Eq. (S6) and Eq. (S7) by

$$\frac{1}{\Psi_h}(T_s - T_h) = \frac{1}{\psi_k}(T_h - T_c) + \frac{\beta ZFA}{(1+m)^2 2d}((2m+1)T_h + T_c)(T_h - T_c) \tag{S8}$$

$$\frac{1}{\Psi_c}(T_c - T_a) = \frac{1}{\psi_k}(T_h - T_c) + \frac{\beta ZFA}{(1+m)^2 2d}(T_h + (2m+1)T_c)(T_h - T_c) \tag{S9}$$

Electric power output per substrate area, $\boldsymbol{w}$ [W/m^2] is written and transformed as,

$$w = (I^2 mR)/A = \frac{m\sigma S^2 F}{(1+m)^2 d}(T_h - T_c)^2 = \frac{mZ}{(1+m)^2}\frac{\beta F}{d}(T_h - T_c)^2 \tag{S10}$$

Temperature difference across the thermoelement relative to the system boundary conditions can be found as,

$$\frac{(T_h - T_c)}{(T_s - T_a)} = \frac{\psi_k}{\psi_k + \frac{q_h}{q_k}\Psi_h + \frac{q_c}{q_k}\Psi_c} \tag{S11}$$

By following Fourier law,

$$q_k = \frac{(T_h - T_c)}{\psi_k} \tag{S12}$$

Since $q_h = \frac{1}{\Psi_h}(T_s - T_h)$, rewriting Eq. (S8),

$$q_h = q_k + \frac{Z}{(1+m)^2}\frac{\beta FA}{2d}((2m+1)T_h + T_c)(T_h - T_c) \tag{S13}$$

Similarly for Eq. (S9),

$$q_c = q_k + \frac{Z}{(1+m)^2}\frac{\beta FA}{2d}(T_h + (2m+1)T_c)(T_h - T_c) \tag{S14}$$

Substituting Eq. (S13) and Eq. (S14) into Eq. (S11)

$$\frac{(T_h - T_c)}{(T_s - T_a)} = \frac{\psi_k}{\psi_k + \left(1 + \frac{1}{q_k}\frac{Z}{(1+m)^2}\frac{\beta FA}{2d}((2m+1)T_h + T_c)(T_h - T_c)\right)\Psi_h + \left(1 + \frac{1}{q_k}\frac{Z}{(1+m)^2}\frac{\beta FA}{2d}(T_h + (2m+1)T_c)(T_h - T_c)\right)\Psi_c} \tag{S15}$$

From Eq. (S3) and Eq. (S12)

$$\frac{(T_h - T_c)}{(T_s - T_a)} = \frac{d}{d + \beta FA\left\{\left(1 + \frac{Z}{2(1+m)^2}((2m+1)T_h + T_c)\right)\Psi_h + \left(1 + \frac{Z}{2(1+m)^2}(T_h + (2m+1)T_c)\right)\Psi_c\right\}} \tag{S16}$$

Eq. (S9) is reformulated with Eq. (S16),

$$w = \frac{mZ}{(1+m)^2}\frac{\beta F}{d}\frac{d^2}{\left[d + \beta FA\left\{\left(1 + \frac{Z}{2(1+m)^2}((2m+1)T_h + T_c)\right)\Psi_h + \left(1 + \frac{Z}{2(1+m)^2}(T_h + (2m+1)T_c)\right)\Psi_c\right\}\right]^2}(T_s - T_a)^2 \tag{S17}$$

Therefore,

$$w = \frac{mZ}{(1+m)^2}\frac{d\beta F}{\left(d + \beta FA\sum \Psi\kappa\right)^2}(T_s - T_a)^2 \tag{S18}$$

where,

$$\sum \Psi = \Psi_h + \Psi_c \tag{S19}$$

and κ is a dimensionless factor shown as,

$$\kappa = \left(1 + \frac{Z}{2(1+m)^2}\left((2m+1)T_h + T_c\right)\right)\frac{\psi_h}{\sum\Psi} + \left(1 + \frac{Z}{2(1+m)^2}\left(T_h + (2m+1)T_c\right)\right)\frac{\psi_c}{\sum\Psi} \quad \text{(S20)}$$

By co-optimization for the factor $\boldsymbol{m}$ and $\boldsymbol{d}$ for maximizing $\boldsymbol{w}$, which is found by taking the derivative of $\boldsymbol{w}$ to be zero, the optimum leg length $\boldsymbol{d_{opt}}$ is found as

$$d_{opt} = \kappa\beta FA\sum\Psi \quad \text{(S21)}$$

Eq. (S21) clearly shows that $\boldsymbol{\kappa}$ at the maximum power output is the optimum ratio of internal thermal resistance to the external thermal resistance. This means thermal impedance match.

$$\kappa = \frac{\psi_k}{\sum\Psi} \quad \text{(S22)}$$

The maximum power output per unit area can be found by applying Eq. (S21) to Eq. (S18) and it becomes a simple formula,

$$w_{\max} = \frac{mZ}{4(1+m)^2}\frac{1}{A\sum\Psi}(T_s - T_a)^2 \quad \text{(S23)}$$

It is important to note that the fractional area factor $\boldsymbol{F}$ disappears in the maximum power output expression (Eq. (S23)). This is the key for the later consideration that reducing fill factor $\boldsymbol{F}$ can lower material usage while maintaining a high power output. At the single point co-optimum, both the electrical and thermal impedance match. We have verified this singularity by the calculations with wide variety of parameters. The electrical impedance match is found to be exactly the same as the conventional expression as

$$m = \sqrt{1 + ZT} \quad \text{(S24)}$$

At the special case $\boldsymbol{\Psi_h = \Psi_c}$ (symmetric thermal resistance) at the co-optimum, from Eq. (S20),

$$\kappa = \left(1 + \frac{ZT}{(1+m)}\right) = m \quad \text{(S25)}$$

Here, $\boldsymbol{T}$ is the mean temperature between two junctions of the leg, $\boldsymbol{T=(T_h+T_c)/2}$. Eq. (S25) shows that the optimum condition is found when $\boldsymbol{\kappa}$ and $\boldsymbol{m}$ are exactly the same but only for the symmetric system.

The external thermal resistance includes the spreading/constriction thermal resistance in the TE substrate due to the fractional area coverage (fill factor). Fig. S2 shows the example of full optimization for the case $\boldsymbol{ZT}$=1 and symmetric thermal resistances ($\boldsymbol{\Psi_h = \Psi_c}$).

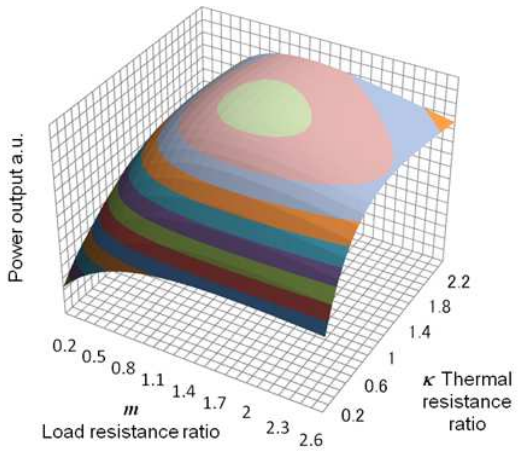

Fig. S2. Full optimization of the power output. m: electrical resistance ratio and κ: leg thermal resistance ratio for F=1, ZT=1, symmetric thermal resistances. The peak is found at m=κ=1.414

SPREADING THERMAL RESISTANCE

Typically, the legs do not occupy the whole foot print of the substrate. Since small fraction of fill factor reduces the heat flow cross section area, spreading/constriction thermal resistance should be taken into account. The thermal resistance is not just a linear function of the fractional area. Fig. S3 shows the cross section of the thermal spreading in the substrate .

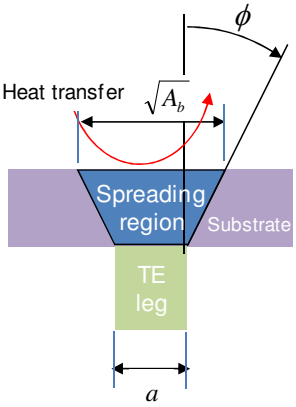

Fig. S3. Thermal spreading by fraction of fill area (cross section view)

In the electronics industry, the spreading thermal resistance model by Song et.al. (Ref. S1) has been commonly used. The model is proven to be in a few percents error compare to the exact theoretical solution. Despite the good engineering accuracy, we cannot make clear the boundaries of the heat spreading region A_b by this model. To build in our analysis, we utilized another model which can make clear the boundary of spreading limit up to 46.45 deg angle for smaller fractions (Ref. S2). One should note this model underestimates the thermal resistance due to the assumption of uniform temperature at heat transfer surface. The range of the error compare to above Song's model

depends on the conditions, but was found within 25% when the fill factor is less than 10%. By following (Ref. S2), the spreading thermal resistance is written as,

$$\psi_{sh} = \psi_{sc} = \frac{\lambda}{\beta_s a(1 + 2\lambda \tan\phi)} \tag{S26}$$

where,

$$\begin{cases} \phi = 5.86\ln(\lambda) + 40.4 & 0.0011 < \lambda \le 1 \\ \phi = 46.45 - 6.048\lambda^{-0.969} & \lambda \ge 1 \end{cases} \tag{S27}$$

and,

$$\lambda = d_s / a \tag{S28}$$

where, $\boldsymbol{a}$ is a feature leg width as defined as,

$$a = \sqrt{FA} \tag{S29}$$

Substrate thickness $\boldsymbol{d_s}$ and its thermal conductivity $\boldsymbol{\beta_s}$ play significant roles in the spreading thermal resistance. For small fractional coverage, the area outside of the spreading region does not influence the heat flow in the thermoelectric elements. Thus, it is natural to consider packing of the elements until the boundaries of the spreading regions touch each other. The limit condition can be expressed as,

$$F = \left(1 - \frac{2d_s \tan\phi}{a}\right)^2 \tag{S30}$$

It is quite important to place the legs packed in the substrate area as, if not, there will be heat losses between the hot and cold reservoirs in the inactive regions. It is very useful to use an analytic model for the system optimization since the spreading region is a strong function of the geometry and the boundary conditions. It will be very slow to use numerical calculations as a function of many parameters.

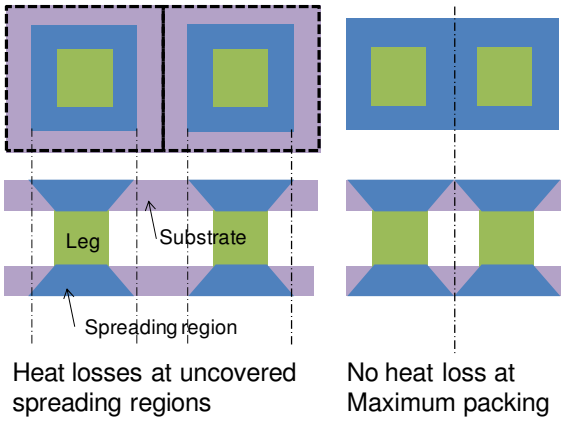

Fig. S4. Leg packing showing the thermal spreading region

POWER OUTPUT WITH FRACTIONAL COVERAGE OF TE ELEMENT

To take into account the spreading resistances, the sum of external thermal resistances Eq (S19) is replaced by Eq (S31).

$$\sum \Psi = \Psi_h + \Psi_c + \frac{2\lambda}{\beta_s a(1 + 2\lambda \tan\phi)} \qquad \text{(S31)}$$

Output power density as a function of fractional coverage (fill factor) is shown in Fig. S5. As expected earlier the power output is nearly independent from the fill factor at 1% or larger. The output gradually decreases as the fill factor decreases to less than 1% due to the limited available heat transport.

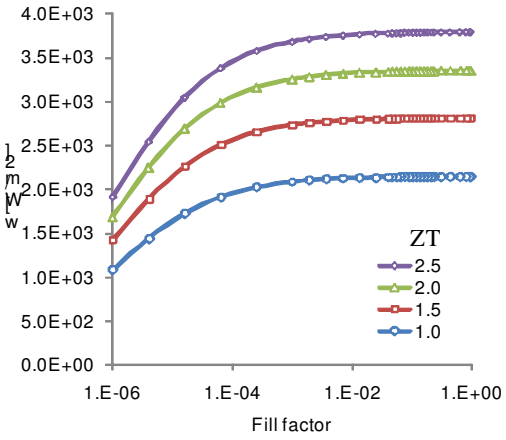

Fig. S5. Power density versus fill factor for different ZT when T_s=600 [K], T_a=300 [K], β_s=140 [W/mK], d_s=0.2e-3 [m], U_h, U_c= 500 [W/m^{2}K]

HEAT SINK OTPIMZATION

There is a significant amount of work on heat sink optimization as described e.g. in (Refs. S3, S4). In this study, the model of Yazawa et al. (Ref. S5) is used, but slightly modified to be able to do a systematic calculation of the energy payback. As shown in Eq. (S23), smaller thermal resistance results in larger power output. At the same time we need to increase the pumping power to the coolant in order to obtain smaller thermal resistances. This results in additional power which is consumed. Thus, the payback analysis is necessary to find the net maximum power output in a realistic system. We assume a heat sink where the fluid path is made of parallel channels as shown in Fig. S6. This structure corresponds to both air convection cooling and water cooling. The water cooled micro channels are typically designed taking the wall thickness to be constant (b) and varying the channel width (fin gap, δ). Since the smaller mass of the heat sink fins is important, the wall thickness is assumed to be the manufacturable minimum.

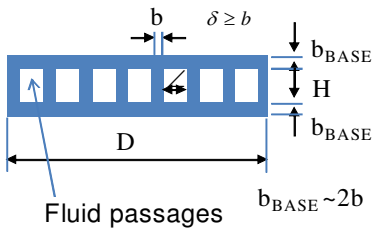

Fig. S6. Heat sink model

In this section, we will optimize the channel design for a given thermal resistance to minimize the pumping power. From the discussion in (Ref. S6), the optimum condition can be found when the convection from the fin surface matches to that of the temperature sensitive fluid flow. The impedance matching condition is described as,

$$U_{BASE}A_{BASE} = 1/\left(\frac{1}{2\dot{m}C_p} + \frac{1}{U_{fin}A_{fin}}\right) \tag{S32}$$

where,

$$A_{fin} = 2N(H+\delta)L \quad and \quad \dot{m} = \rho N\delta H u \tag{S33}$$

From the heat transfer match, $\boldsymbol{u}$: flow velocity is found as:

$$u = \frac{N_u\beta_f}{2\rho C_p}\left(\frac{H+\delta}{H\delta}\right)^2 L \tag{S34}$$

By combining above with the Eq (S32), $\boldsymbol{U_{BASE}}$: heat transfer coefficient at foot print is found as:

$$U_{BASE} = \frac{N_u\beta_f(H+\delta)^2}{2H\delta(b+\delta)} \tag{S35}$$

This equation can be solved in order to determine the optimum $\boldsymbol{\delta}$ channel spacing.

$$\delta = H\frac{(bx-1)-\sqrt{(1-bx)^2-(1-2Hx)}}{(1-2Hx)} \tag{S36}$$

where,

$$x = \frac{U_{BASE}}{N_u\beta_f} \tag{S37}$$

In above relation, $\boldsymbol{Nu}$ is Nusselt number and $\boldsymbol{D_h}$ is the hydraulic diameter which is based the dimensionless heat transfer coefficient and determined by aspect ratio $\boldsymbol{\delta/H}$ as shown in Eq (S38). Here we followed the data of Kays and London (Ref. S7). We assume constant wall temperature and fully developed flow for entire channel.

$$Nu = 4.52(1-\delta/H)^{3.78} + 2.98 \tag{S38}$$

Pumping power w_{pp} required for this configuration is determined by:

$$w_{pp} = \frac{Nu\delta H\Delta P_{\mathrm{ch}}}{A_s} \qquad \text{(S39)}$$

Volume flow rate is found straight forward by the product of mean velocity and cross section area. The other component is pressure loss throughout the channel flow ΔP_{ch} which is given by:

$$\Delta P_{\mathrm{ch}} = \frac{K\rho}{2}u^2 + \frac{48\mu L}{D_h^{\,2}}u \qquad \text{(S40)}$$

The previous model is valid when the fluid flow regime is laminar. Since the channel wall thickness is small compare to the channel spacing, the first term of Eq (S40) can be neglected and the velocity dependence becomes linear. Substituting this simplified Eq (S40) and Eq (S34) into Eq (S39), the pumping power as a function of channel spacing is found as:

$$w_{pp} = 3\mu\left(\frac{N_u\beta_f}{\rho C_p}\right)^2 \frac{(H+\delta)^6}{(b+\delta)(H\delta)^5}L^2 \qquad \text{(S41)}$$

Finally, the optimum channel spacing δ is found by Eq (S36) and the required pumping power is determined by Eq (S41).

REFERENCES

(S1). Song, S.; Lee. S.; Au, V. Closed-Form Equation for Thermal Constriction/Spreading Resistances with Variable Resistance Boundary Condition, *Proc. of IEPS 1994 International Electronics Packaging Conference*, **1994**, 111-121.

(S2) Vermeersch, B.; De Mey, G. A Fixed-Angle Dynamic Heat Spreading Model for (An) Isotropic Rear-Cooled Substrates, *ASME Journal of Heat Transfer*, **2008**, *130*(12), 121301.

(S3) Murakami, Y.; Mikic, B.B. Parametric Optimization of Multichanneled Heat Sinks for VLSI Chip Cooling, *IEEE Transaction on Components and Packaging Technologies*, **2001**, *24*(1), 2-9.

(S4) Teertstra P.; Culham, J.R.; Jovanovich, M.M. Analytic Modeling of Forced Convection in Slotted Plate Fin Heat Sinks, *Proceedings of 1999 ASME International Mechanical Engineering Congress and Exposition*, **1999**, *364*(1), 3-11.

(S5) Iyengar, M.; Bar-Cohen, A. Least-Energy Optimization of Air-Cooled Heat Sinks for Sustainable Development, *IEEE CPT Transactions*, **2003**, *26*(1), 16-25.

(S6) Yazawa K.; Solbrekken, G.L.; Bar-Cohen, A. Thermofluid Design of Energy Efficient and Compact Heat, *Proceedings of 2003 International Electronic Packaging Technical Conference and Exhibition*, **2003**, IPACK2003-35242.

(S7) Kays and London, 'Fig. 6-3 Nusselt numbers for laminar flow in rectangular tubes with fully developed velocity and temperature problems', In *Compact heat exchanger 3rd edition,* 1984, Krieger publishing, Malabar, Florida.